Okra (Abelmoschus esculentus) *Fibre Based PLA Composites: Mechanical Behaviour and Biodegradation*

E. Fortunati, D. Puglia, M. Monti, C. Santulli, M. Maniruzzaman, M. L. Foresti, A. Vazquez & J. M. Kenny

Journal of Polymers and the Environment
formerly: `Journal of Environmental Polymer Degradation'

ISSN 1566-2543

J Polym Environ
DOI 10.1007/s10924-013-0571-5

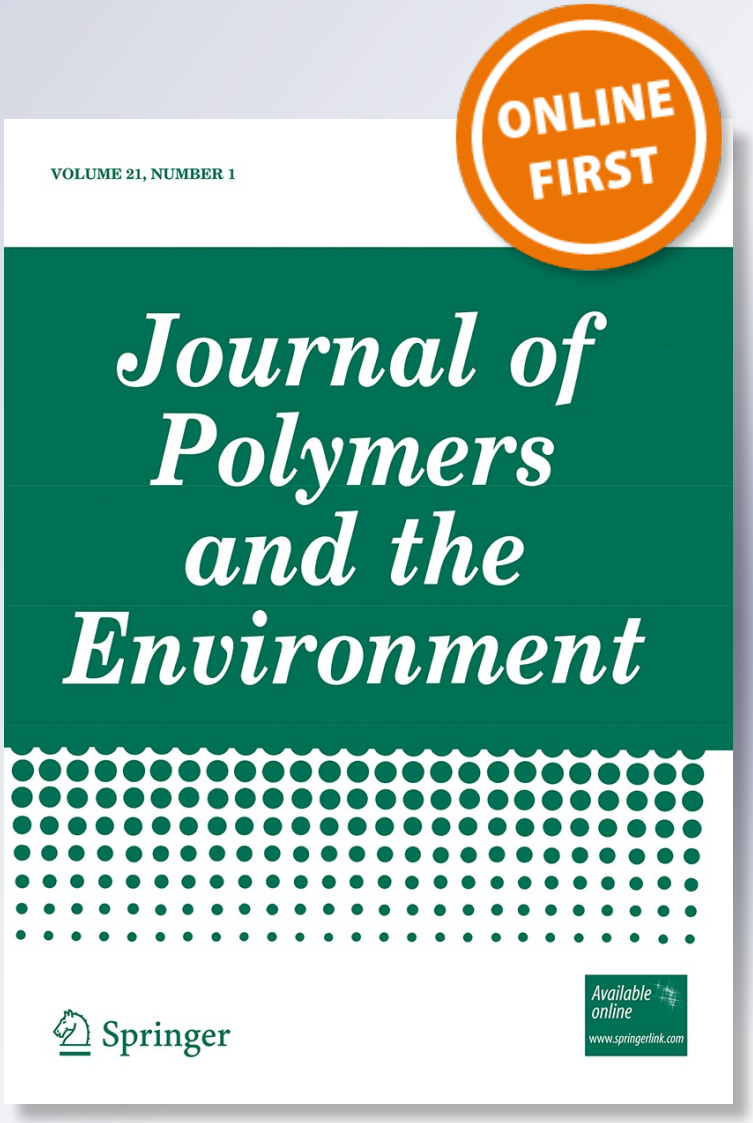

J Polym Environ
DOI 10.1007/s10924-013-0571-5

ORIGINAL PAPER

Okra (*Abelmoschus esculentus*) Fibre Based PLA Composites: Mechanical Behaviour and Biodegradation

E. Fortunati · D. Puglia · M. Monti · C. Santulli · M. Maniruzzaman · M. L. Foresti · A. Vazquez · J. M. Kenny

Abstract Okra (Lady's finger, *Abelmoschus esculentus*) fibres were introduced in a poly(lactic) acid (PLA) polymer matrix as short fibres (5–10 mm), in amounts variable between 10 and 30 %wt. For this purpose, both untreated and alkali treated okra fibres were used. The obtained composites, in view of the envisaged application for sustainable packaging purposes, has been tested morphologically, mechanically and subjected to chemical characterisation, while the biodegradation profile has been studied. The introduction of fibres in the polymer matrix always resulted in a higher stiffness of the obtained composite. The addition of okra fibre to PLA results in an increased ability of the PLA matrix to crystallize due to the nucleation effect of the okra fibre, and this effect was more evident in the composites produced with alkali treated fibres. The biodegradation process was accelerated by the addition of higher contents of fibres into the composites due to preferential degradation of the fibres themselves: this effect was increased when composite fibres are alkali-treated.

E. Fortunati · D. Puglia (✉) · M. Monti · J. M. Kenny
Civil and Environmental Engineering Department, University of Perugia, UdR INSTM Strada di Pentima 4, 05100 Terni, Italy
e-mail: dpuglia@unipg.it

C. Santulli
Chemical Engineering, Materials and Environment Department, Sapienza University of Rome, Via Eudossiana 18, 00184 Rome, Italy

M. Maniruzzaman
Department of Applied Chemistry and Chemical Technology, Islamic University, Kushtia 7003, Bangladesh

M. L. Foresti · A. Vazquez
CONICET-INTECIN-FIUBA, Facultad de Ingeniería, Universidad de Buenos Aires, Buenos Aires, Argentina

Keywords Poly(lactic) acid · Okra fibre · Alkali treatment · Biodegradation

Introduction

Okra bahmia (*A. esculentus*), also known as Lady's finger, is a monocotyledon herbaceous plant of the Malvaceae family, present mainly in the Indian region, but also in the Mediterranean area and in Brazil. From okra bark, fibres can be extracted, of some use in the food sector, as an added nutrient in gums and pectins. The recent study of their thermal and mechanical behaviour indicated okra fibres as a possible candidate for the use in the production of biodegradable composites [1], also in view of the maximum length of the extracted fibres, which is in excess of 60 cm [2]. The principal question would be, nonetheless, understanding whether it is possible to use these fibres not just as a waste material, but ideally to offer some reinforcement to a biodegradable, polymer matrix. This would be done with the idea of providing some application for the obtained composite e.g., in the packaging sector. This is suggested by the fact that previous studies did not demonstrate that most common chemical treatments, such as bleaching or alkalization, substantially improve the fibre properties, so that in the end the variability of their mechanical properties would remain far too high for their possible use in structural composites [3, 4]. In this respect, one possibility that has been recently explored and showed some potential is the extraction of nanocellulose from okra fibres and its introduction in a polyvinyl alcohol matrix [5]. Biopolymers, including poly(lactic) acid (PLA), showed a significant potential to be coupled to produce truly green composite materials: in particular, some work carried out refers to materials for

Published online: 17 February 2013

semi-structural use, usually based on bast fibres, such as kenaf [6–8], jute [9, 10], hemp [11–13], flax [14–16]. In some cases, the production of these composites has an additional significance in the fact of assisting the reviving of a local fibre market, such as for phormium [17], or proposing more extensive cropping for spontaneously growing plants, such it is the case for nettle [18].

On a lower profile, which can be recommended for materials aimed at large volume applications, where the compostability is a fundamental requirement, can be the use of easily available biomass, such as herbaceous plants, hardly appropriate for the production of textiles, to be coupled with the biodegradable polymer. In this case, the use of short fibres is also recommendable, in particular because the large presence of defects and the uneven fibre diameter results in a rather ineffective stress transfer and as a consequence in lower mechanical performance of the composite for fibres exceeding 5–10 mm length [19–21].

This work on okra fibres as reinforcement in PLA biodegradable matrix also enters in the latter domain and it is aimed at the possible use of this material in the packaging field. A disintegration test in composting condition has been also performed, with the same procedure followed recently on other PLA composites, filled with phormium leaf fibres in order to have useful information about the post-use of the studied composite systems [22]. Leaf fibres have generally a lower mechanical strength if compared to bast fibres and their mechanical performance can change from one crop to another depending on the particular climate condition during the year. In order to verify the possibility to obtain a fibre which was less related to the year of the crop and from the area where it comes from, in this paper we have also performed a fibre chemical alkali treatment, in order to compare the results obtained with the pristine fibres (hereinafter referred to as UOF–untreated okra fibres) with the treated ones (hereinafter referred to as ODC–okra derived cellulose).

Experimental

Materials

Okra (*A. esculentus*), whose local name is Dherosh, is a monocotyledon plant. The plant has been collected in Kushtia District (Bangladesh). After collection, the fresh plant was kept under water to allow microbial degradation. Within 15–20 days the stems degraded sufficiently to enable fibre extraction. The fibres were isolated from the degraded stems by being washed three times using deionized water. They were then tied with ropes, dried in open air and kept in moisture-proof container afterwards [4].

Poly(lactic) acid (PLA) 3051D (specific gravity 1.25 g/cm^3, molecular weight 1.42×10^4 g/mol, MFI of 7.75 g/10 min (210 °C, 2.16 kg), melting temperature of 170 °C) was supplied by Nature Works®, USA.

Okra Fibre Treatment

Okra fibres were washed with distilled water numerous times and dried 24 h at 80 °C. They were then chopped to an approximate length of 5-10 mm and de-waxed boiling in a mixture toluene/ethanol (2:1 volume/volume) for 6 h. The fibres were filtered, washed with ethanol for 30 min and dried. Subsequently, the fibres were subjected to a treatment procedure for removing the amorphous fraction of the raw fibres. Firstly okra fibres were treated with 0.7 wt%/v of sodium chlorite $NaClO_2$; the fibres (liquor ratio 1:50) were boiled for 2 h and the solution pH was lowered to about 4 by means of acetic acid for the bleaching. A treatment with sodium bisulphate solution at 5 wt%/v was carried out and at the end of this preliminary chemical process, holocellulose (α-cellulose + hemicellulose) was obtained, by the gradual removal of lignin [23]. The holocellulose was treated with 17.5 wt%/v of NaOH solution, filtered and washed with distilled water. The obtained cellulose fibres were dried at 60 °C in a vacuum oven until constant weight.

Composite Production

The PLA/okra composites were produced in a co-rotating twin screw microextruder (DSM Explore 5&15 CC Micro Compounder). PLA pellets were dried in a vacuum oven at 100 °C for 3 h and the fibres were dried at 60 °C for 12 h. The processing parameters were tuned in order to optimize material final properties and were eventually set at 50 rpm as screw speed, 1 min mixing time and 165–185–200 °C as temperature profile. The composites were prepared with several amounts of okra fibres: 10, 20 and 30 wt% respect to the polymer matrix, with both pristine (UOF) and alkali treated fibres (ODC). Neat PLA was also injection moulded as a control material.

Characterization Methods

The morphology, shape and diameters of pristine okra fibres (UOF) and okra derived cellulose (ODC) were evaluated by means of a field emission scanning electron microscope (FESEM Zeiss, model Supra 25). The cross-section and longitudinal surfaces were considered and the diameters calculated on a series of fifty fibres for each case.

A morphological analysis on the fracture surface of the produced PLA/okra composites was performed using

FESEM. The fracture surface was obtained by immersing the samples in liquid nitrogen and then impacted. Once produced, it was sputter coated with gold.

The mechanical characterization of the produced composites was performed with a Lloyd Instruments dynamometer (model LR30 K), according to ISO 527 standard. At least 5 specimens per material were tested under tensile loading in order to have good reliability of the results.

Differential scanning calorimeter (TA Instruments, Q200) measurements were performed in the temperature range from −25 to 250 °C, at 10 °C/min, performing two heating and one cooling scans. Melting and cold crystallization temperatures and enthalpies (T_m, T_{cc} and ΔH_m, ΔH_{cc}) and the glass transition temperature (T_g) were investigated from the second heating.

Attenuated total reflectance Fourier transform infrared spectroscopy (ATR-FTIR) characterization of UOF and ODC fibres was carried out using a IR Affinity-1 Shimadzu Fourier Transform Infrared Spectrophotometer equipped with a ZnSe ATR accessory.

The X-ray diffraction patterns (XRD) of UOF and ODC were recorded in a Rigaku diffractometer using a copper K-alpha X-ray source. Scans were obtained from 10° to 100° (2θ) in 0.05° steps at a scanning rate of 0.6°/min.

Biodegradation

Disintegration patterns of PLA and PLA/okra composites were observed through a disintegrability test in composting conditions according to the ISO 20200 standard, which defines as *disintegrated* a sample that achieves in 90 days the 90 % of disintegration: namely, after this period, 10 % only has to be retained in a 2 mm sieve. The test is supposed to simulate a real composting process. A specific quantity of compost, supplied by Gesenu S.p.a., was mixed together with the synthetic biowaste, prepared with certain amount of sawdust, rabbit food, starch, sugar, oil and urea as reported in the relevant aforementioned standard. The water content of the substrate was around 50 wt% and the aerobic conditions were guaranteed by mixing it very slowly. Samples were buried at 4–6 cm depth into an organic substrate and incubated at 58 °C. The incubated materials were recovered at different disintegration steps and washed with distilled water, dried in oven at 37 °C for 24 h, and weighted with an analytical balance. Microstructure of PLA and PLA composites at 10, 20, 30 and 40 days of incubation in composting was investigated by scanning electronic microscopy (FESEM Zeiss, model Supra 25). Photographs of the samples were taken for visual comparison. Fourier infrared spectra of the samples in the 400–4,000 cm^{-1} range, were recorded by a Jasco FTIR 615 spectrometer, in attenuated total reflection mode (ATR).

Results and Discussion

Characterization of Okra Fibres

Figure 1 summarizes morphological and chemical investigations of pristine (UOF) and alkali treated (ODC) okra fibres. FESEM micrograph of the original raw okra fibres and the morphology of the treated okra fibres were reported in Fig. 1a and b, respectively. Pristine okra fibres (UOF) are characterized by a polygonal shape with a diameter of 88.3 ± 27.3 μm (calculated on a series of fifty fibres) [4].

The chemical treatment, while partially removing the amorphous fraction of the fibre, induces a decrease of the diameter. After the treatment it was measured as 9.8 ± 2.9 μm (Fig. 1b). The morphology of the ODC lateral surface shows a quite rough surface, where the roughness mainly oriented in the longitudinal direction.

As previously reported [1], the FTIR spectrum of pristine okra fibres (Fig. 1c) shows the absorption bands characteristic of functional groups present in cellulose, hemicellulose and lignin. The broad absorption band found in the 3,600–3,100 cm^{-1} region and centred at 3,320 cm^{-1} is due to the O–H stretching vibration and hydrogen bond of hydroxyl groups. The peaks at 2,925 and 2,853 cm^{-1} are due to the C–H stretching vibration from CH and CH_2 in cellulose and hemicellulose [24]. The absorbance centred at 1,730 cm^{-1} is assigned to the C=O stretching vibration of the linkage of carboxylic acid in lignin and ester groups in hemicellulose [25, 26]. The band found in the 1,660 –1,560 cm^{-1} can be assigned to the presence of water in the fibres [27]. Moreover, lignin also shows absorption bands in this region due to the aromatic skeletal vibration [28, 29]. The small peak at 1,508 cm^{-1} is attributed to C=C stretching of the aromatic ring of lignin [26, 28]. The absorbance at 1,430 cm^{-1} is attributed to CH_2 symmetric bending [30]. The two peaks observed at 1,366 and 1,320 cm^{-1} in the spectrum are assigned to the bending vibration of C–H and C–O groups of the aromatic ring in polysaccharides [31]. The absorbance peak at 1,237 cm^{-1} corresponds to the C–O stretching vibration of the acetyl group of hemicellulose and lignin [26, 32]. The strong absorption peak at 1,030 cm^{-1} is ascribed to the C–O and O–H stretching vibration which belongs to polysaccharide in cellulose [33]. The peak observed at 894 cm^{-1} which represents the C1 group frequency or ring frequency, is characteristic of β-glycosidic linkages between the sugar units [34]. In the FTIR spectrum of treated okra (Fig. 1c), differences from the untreated fibre arise mainly from bands at 1,728, 1,508 and 1,237 cm^{-1}, which are characteristic of functional groups present in hemicellulose and lignin. The band at 1,728 cm^{-1} attributed to the C = O stretching of the acetyl groups of hemicellulose, is not present in treated samples. The removal of hemicellulose

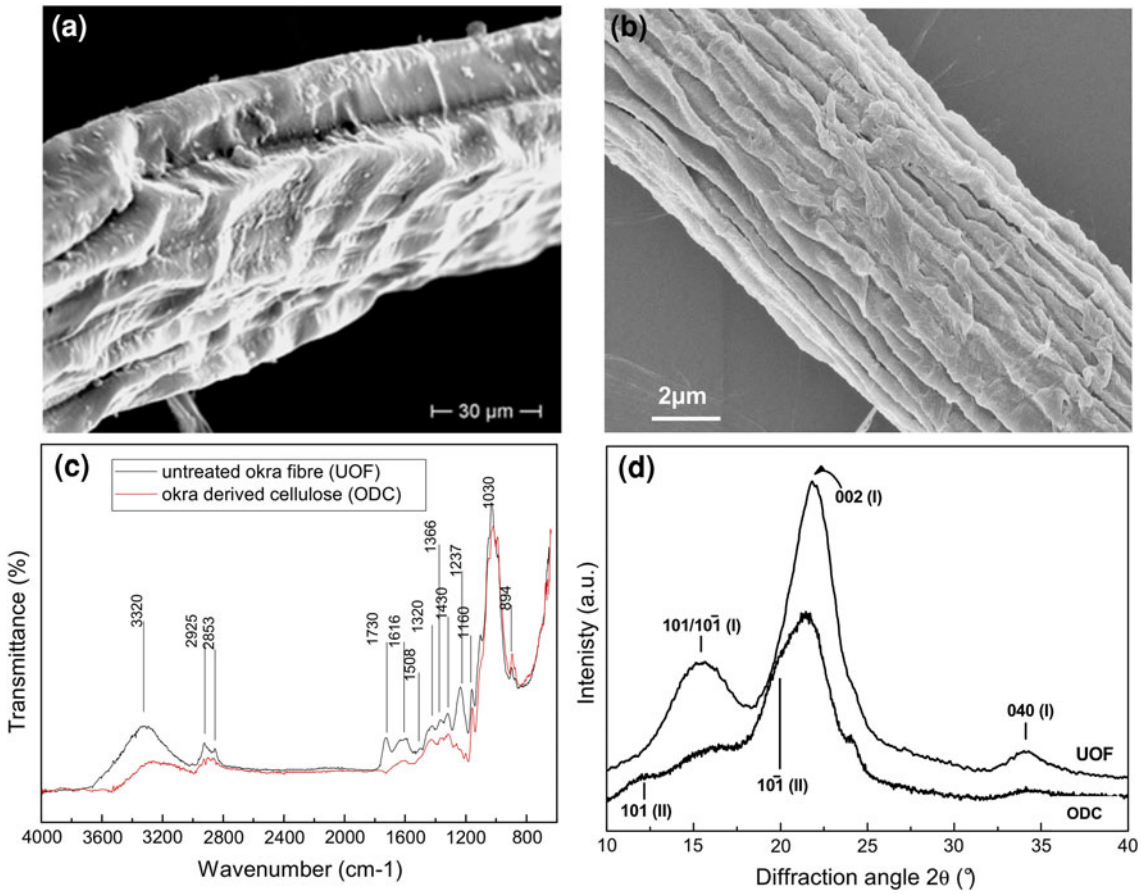

Fig. 1 Morphological and chemical characterization of pristine (UOF) and okra derived cellulose (ODC): FESEM micrograph of the UOF okra fibre (**a**) and ODC fibre (**b**), ATR-FTIR spectra of UOF fibres and ODC (**c**), X-ray diffraction patterns of UOF and ODC fibres (**d**)

from the fibre surfaces causes this peak to disappear. The small peak found at 1,508 cm^{-1} for okra fibres and attributed to C = C stretching of the aromatic ring of lignin, appears only as a very small shoulder in the treated sample, indicating the presence of residual amounts of associated lignin. Treatment of okra fibres also resulted in the reduction in the intensity of the peaks found at 1,239 cm^{-1} (C–O stretching vibration of the acetyl group of lignin and hemicellulose), which also indicated the partial removal of lignin from the fibre surface.

Results from XRD analyses are presented in Fig. 1d. Untreated okra fibre shows diffraction peaks at diffractometer angles centred at 15.6°, 21.8° and 34.0°, which are characteristic of cellulose I [36]. Peaks at 21.8° and 34.0° correspond to 002 and 040 lattice planes of cellulose I, whereas the crystalline peak with a maximum at $2\theta = 15.6°$ results from the overlapping of the characteristic 101 and 10–1 peaks of cellulose I (placed at 14.7° and 16.6°, respectively) [35]. As shown in the UOF diffractogram, these two peaks have combined to form a broad peak, which has been reported to be due to the presence of non-cellulosic materials in the fibres [36, 37].

XRD results of ODC show peaks characteristic of cellulose I and cellulose II. Relative to untreated okra, for ODC the peak at the highest angle has shifted toward lower 2θ values ($2\theta = 21.2°$, indexed 002). The small shoulder at $2\theta = 12.0°$, indexed 101, suggests the presence of cellulose II among treated fibre. Besides, the slight shoulder observed at $2\theta = 19.9°$ can be assigned to the characteristic 10-1 lattice plane of cellulose II. The diffraction intensities of ODC are common among fabrics treated commercially with sodium hydroxide versus untreated yarns [38]. It must be pointed that conversion to cellulose II upon alkali treatment was only partial since the peak between 14.7° and 16.6° (attributed to the overlapping of 101 and 10–1 lattice planes of cellulose I) is still visible; whereas no doublet in the intensity of the main peak is clearly seen. A typical X-ray diffraction profile of cellulose II can be found elsewhere [39].

The crystallinity index (CI) is frequently used to describe the relative amount of crystalline material in cellulose. The CI of celluloses has been measured using several different techniques including XRD, solid-state 13C NMR, infrared (IR) spectroscopy and Raman spectroscopy [40]. In the

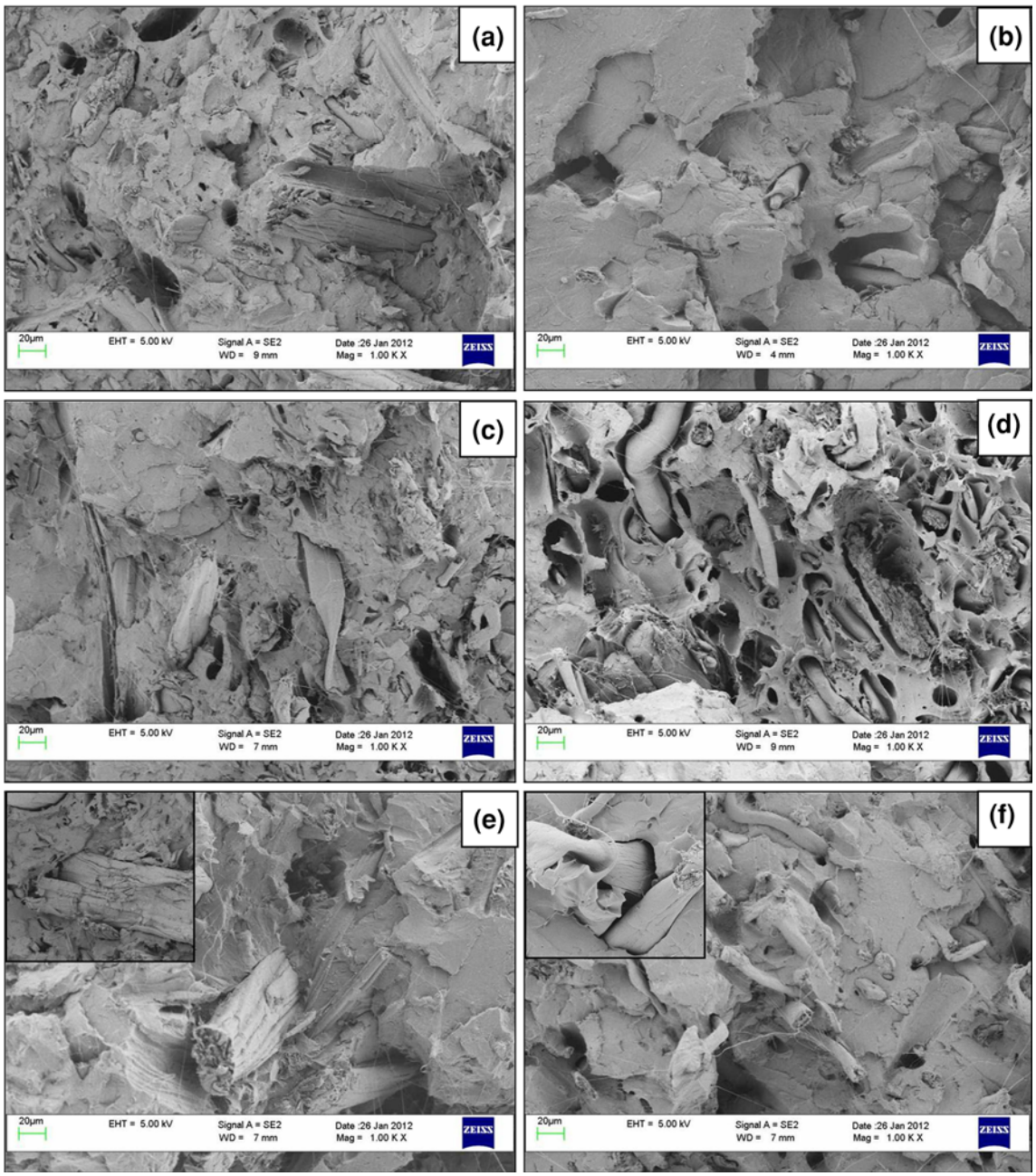

Fig. 2 Fracture surfaces of the produced PLA/okra composites reinforced with 10 wt% of UOF **a** and ODC **b**; 20 wt% of UOF **c** and ODC **d**; 30 wt% of UOF **e** and ODC **f** with insets

current contribution CI of UOF and ODC was calculated as the ratio of crystalline peaks area to the total diffractogram area. The easy and widely used Segal′s XRD peak height method was not used for CI estimation since it has been reported that it cannot be applied to the cellulose II allomorph [40]. Results of the area method showed a CI of 50.6 % for UOF whereas CI of ODC was 49.7 %. Similar CI values found for UOF and ODC can be interpreted as the result of the removal of amorphous non-cellulosic components of okra (which should lead to a CI increase), overlapped with the partial conversion of cellulose I to cellulose II and the consequent loss in crystallinity. Conversion from cellulose I to cellulose II takes place in the amorphous regions and gradually converts crystals of increasingly larger dimensions yielding a more amorphous microstructure [35].

Morphological Analysis of Composites

Figure 2 shows the fracture surface of the produced PLA/okra composites. In particular, Fig. 2a and b show the

Table 1 Mechanical response of neat PLA and PLA/okra composites

Materials	Young's modulus (MPa)	σ_{yield} (MPa)	ε_{yield} (%)	σ_{break} (MPa)	ε_{break} (%)
PLA	2,829 ± 41	58.9 ± 1.9	2.6 ± 0.1	51.5 ± 0.7	4.2 ± 0.6
PLA/10UOF	4,029 ± 368	56.1 ± 2.1	1.9 ± 0.1	55.1 ± 2.3	2.0 ± 0.1
PLA/20UOF	4,149 ± 122	56.2 ± 1.1	1.9 ± 0.1	54.1 ± 1.5	2.2 ± 0.3
PLA/30UOF	4,633 ± 275	58.8 ± 1.4	1.9 ± 0.2	58.4 ± 1.9	1.9 ± 0.2
PLA/10ODC	3,431 ± 155	54.3 ± 2.1	2.1 ± 0.1	48.6 ± 1.9	2.7 ± 0.4
PLA/20ODC	3,985 ± 138	54.5 ± 2.3	1.9 ± 0.1	51.7 ± 1.6	2.1 ± 0.2
PLA/30ODC	3,861 ± 167	55.3 ± 2.4	1.9 ± 0.1	53.4 ± 2.8	2.1 ± 0.3

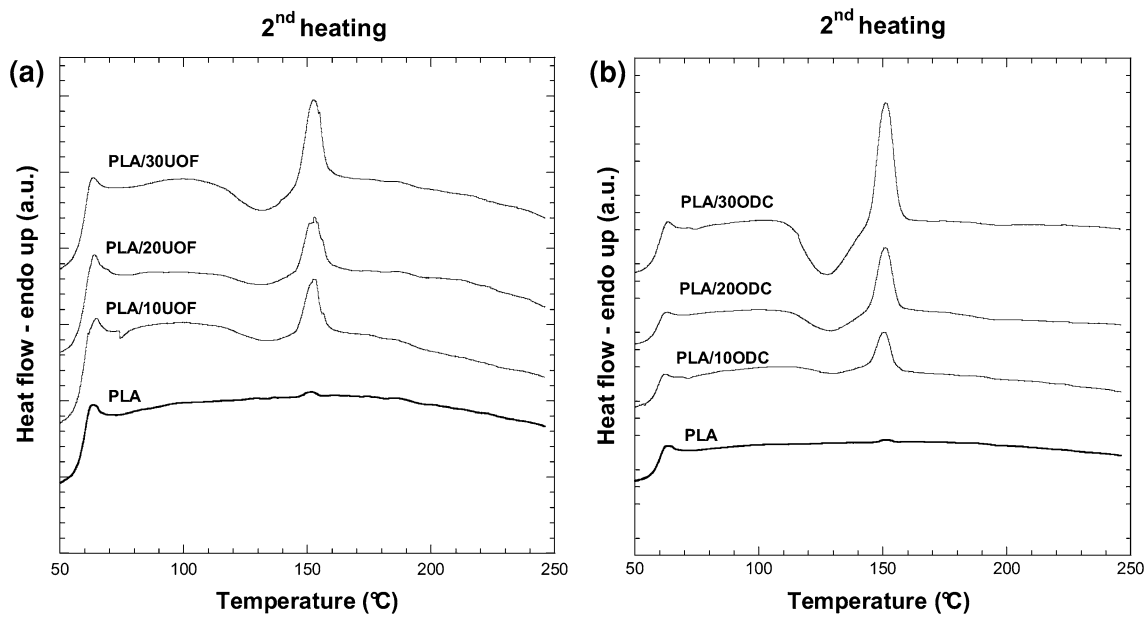

Fig. 3 Dynamic DSC scans (second heating) of all systems loaded with different content of UOF (**a**) and ODC (**b**)

composites reinforced with 10 wt% of UOF and ODC respectively; Fig. 2c and d show the composites reinforced with 20 wt% of UOF and ODC respectively; Fig. 2e and f show the composites reinforced with 30 wt% of UOF and ODC respectively. A general homogeneous distribution of the fibres in the PLA matrix was obtained during the extrusion process with both the pristine and treated fibres. Paying attention to the fibre/matrix interphase, it can be pointed out that the pristine fibres seem to have a stronger adhesion with the matrix with respect to the treated ones. This can be due to the fact that, although the treated fibres show a quite rough surface (see Fig. 1b), the more pronounced roughness of the raw fibres can assure a more intense physical bond with the matrix.

Mechanical Characterization

In Table 1 the results of the mechanical characterization were reported in terms of Young's modulus, yield stress, strain at yield stress, stress and strain at break. As it is possible to observe, the stiffness significantly increases for all the produced composites accordingly with the fibre fraction, while all the composites show a strong reduction in the plastic deformation, regardless of whether the fibres are treated or not.

The Young's moduli of the composites are all higher than that of neat PLA, which is likely to be due to the constraint of the matrix by the fibre at low loads. Mathew et al. [41] reported that cellulose reinforcement increased the crystallinity of PLA. These crystalline regions would contain increased physical cross-links and therefore could be contributing to the increase in the measured Young's moduli; at the same time, the increased crystallinity of PLA, due to cellulose reinforcement, could result in more brittle PLA limiting the tensile strengths of the composites. Absorbed moisture could also cause degradation of PLA by hydrolysis during processing at higher temperature, resulting in a possible reduction in interfacial strength and as a consequence, composite tensile strength. This could also have limited the strength of the alkali treated short fibre composites.

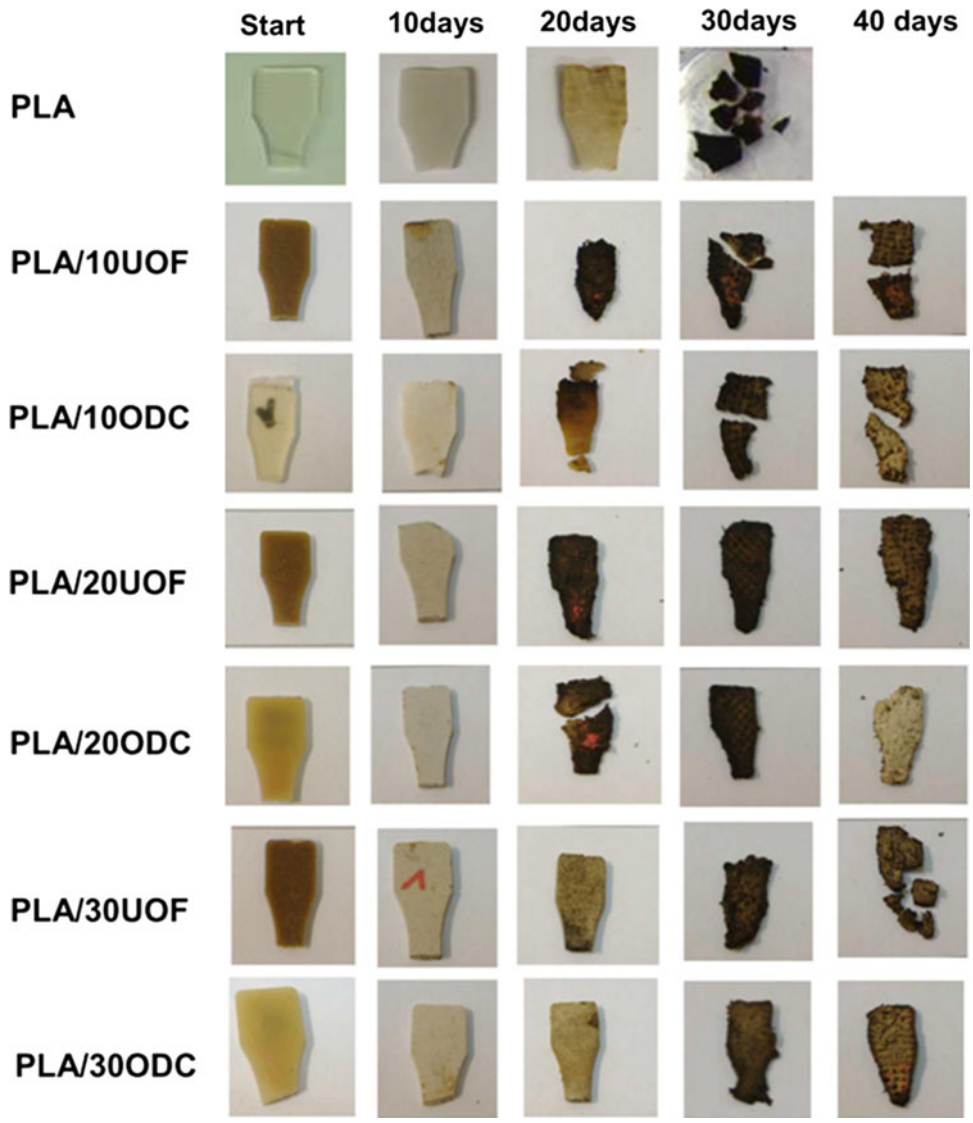

Fig. 4 Photographs of neat PLA and PLA/okra composites at different incubation times

With respect to the yield stress, just a general slight decrease can be observed for all the studied materials, highlighting the presence of a weak fibre/matrix interphase. As for this property, the treated fibres show lower values than the UOF. Although the smaller diameter of the treated fibres confers a higher surface-to-volume ratio, which should allow a better interaction between fibre and matrix, the interaction and therefore the stress transfer between the fibres surface and the PLA matrix become weaker after the alkali treatment [42]. This weak interphase was already underlined in the morphological analysis, where FESEM images (see especially insets Fig. 2e, f) evidenced that the ODC are not strongly connected with the matrix, presenting de-bonding of the fibres much more pronounced if compared to UOF composites.

Thermal Behaviour

Differential scanning calorimetry was used to investigate the glass transition, crystallization and melting phenomena of PLA and PLA/okra composites in relation to the fibre content and to the effect of fibre chemical treatment. Figure 3 summarizes the dynamic DSC behaviour during the second heating scan of all systems loaded with different content of UOF (Fig. 3a) and ODC (Fig. 3b).

The heating thermograms for PLA matrix displayed successively the glass transition temperature (T_g), with a sharp endothermic peak associated to the T_g, typically attributed to stress relaxation on heating [43], and a less evident melting endotherm peak at T_m. The T_g was about 60 °C, and the endothermic peak was detected at about

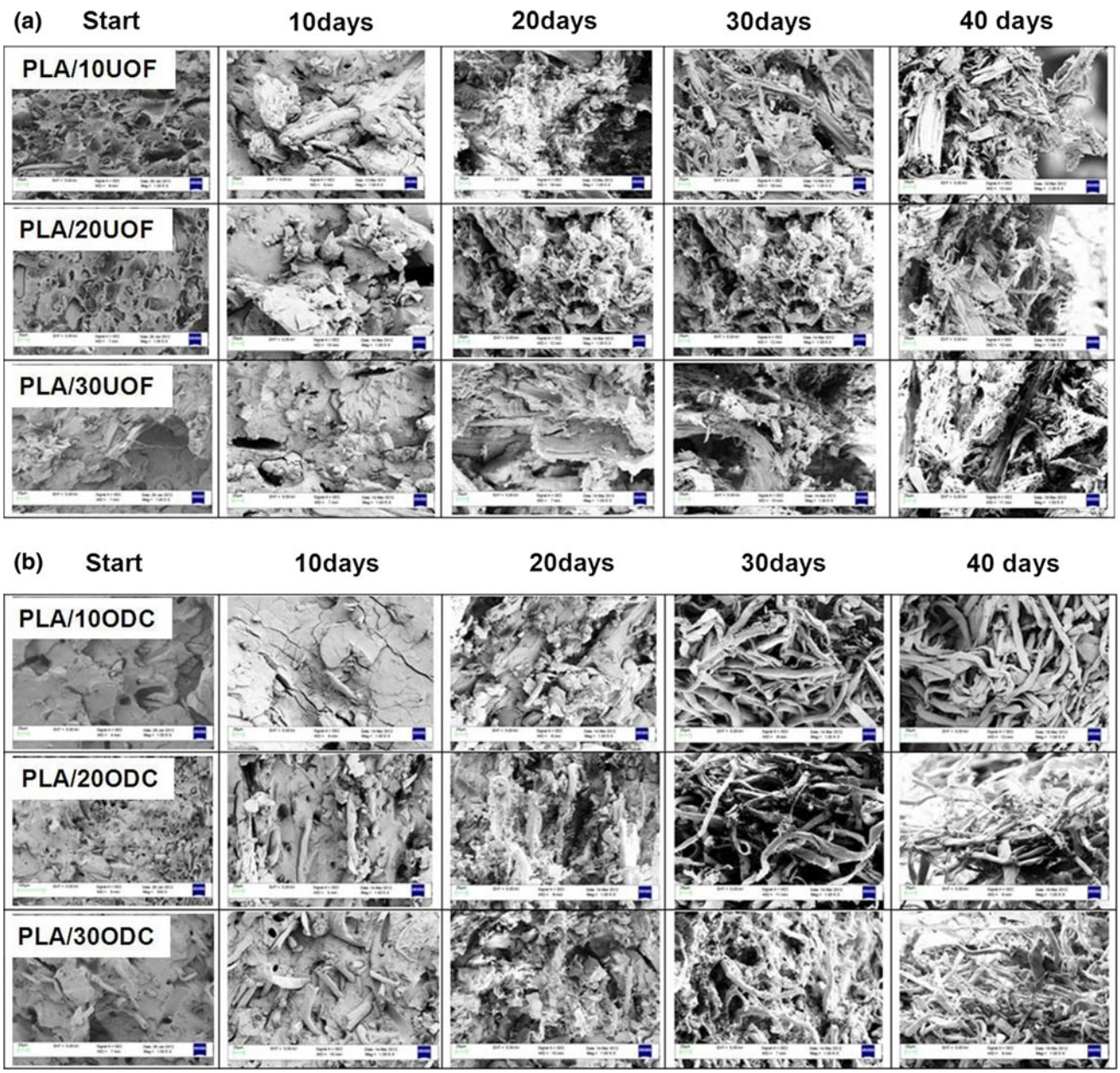

Fig. 5 FESEM observations conducted on PLA/okra after different steps of incubation for both UOF (**a**) and ODC (**b**) based systems

150 °C [44, 45]. We have previously studied the crystallization behavior of this PLA [47]. Although semi-crystalline, the PLA 3051D was reported to have a slow nucleation and crystallization rates such that the sample would be amorphous after normal quenching [46]. We have proved that with the increase of the heating rates, the cold crystallization temperature (T_{cc}) is very hard to be observed in PLA based systems. Under fast heating conditions, the amorphous PLA chains do not have enough time to well self-adjust, resulting in reduced cold crystallization [45].

The thermograms for the PLA/okra composites show the glass transition temperature, the melting endotherm and a well evident cold crystallization exotherm (T_{cc}) that becomes more evident with fibre content; the highest values of cold and melting enthalpies, respect to the amorphous PLA matrix, were also detected in the case of PLA loaded with 30 wt% of reinforcement in both untreated and okra derived cellulose based systems. The addition of okra fibres to PLA suggested possible induced crystallization phenomena during the heating scan and this effect was more evident in the composites reinforced with strong

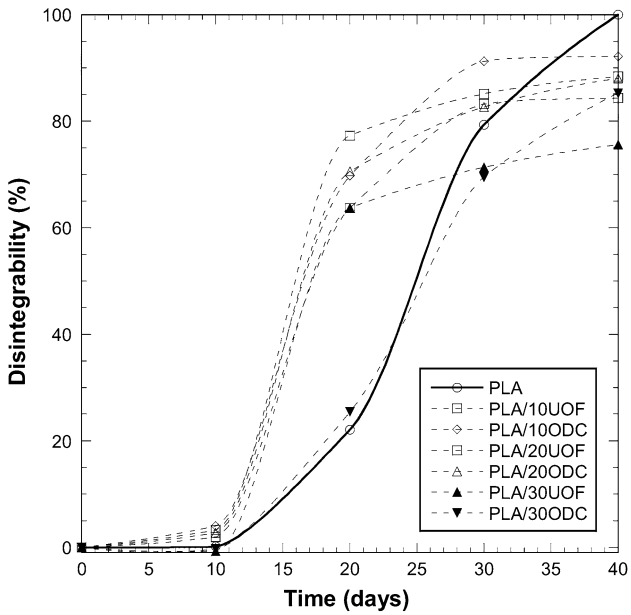

Fig. 6 Disintegration curves of neat PLA and PLA/okra composites

alkali treated fibres (where non-cellulosic surface components such as lignin and hemicelluloses were removed) that showed a more intense cold crystallization peak, highlighting a different capability of these systems to re-crystallize. As a result of the modification of fibre surfaces by alkali treatment, bond ability between the fibre and PLA matrix is improved due to increased interaction by potential hydrogen bonding and mechanical interlocking between them. The increased interaction of the fibre with the PLA matrix could further help the fibre surface to act as nucleation sites for the crystallization of PLA. This promotes the growth and formation of transcrystalline regions around the fibre normal to the fibre surface [47].

Biodegradation

Disintegrability in composting conditions was first evaluated by visual observation of the PLA and PLA/okra composites. The effects of gradual decomposition of neat PLA and PLA/okra composites with different fibre volumes during their soil burial test for times up to 40 days are depicted in Fig. 4. The results presented here clearly indicate that the investigated materials were subject to biodegradation by incubation with compost and the kinetics and dynamics of the mineralization processes depended on the nature and chemical characteristics of the materials. Moreover, the compost appeared to provide a very suitable environment for the biodegradation of such materials. Indeed, its high temperature and relative humidity may have facilitated the hydrolytic degradation of the tested polyester, inducing fundamental microstructural changes and molecular rearrangements [48]. Figure 4 shows that all samples start to change their colour becoming more opaque after yet 10 days of incubation, while they exhibited a considerable surface deformation with the presence of evident fractures starting from 20 days in composting. This effect at 20 days of incubation was more evident in the case of composites based on 10 and 20 wt% of both untreated and treated okra fibres while a more stable behaviour was detected in the systems loaded with 30 wt% of okra fibres that show an intact surface at 20 days of incubation. The changes in sample colour could be a signal that the hydrolytic degradation process of the polymer matrix has started, thus inducing a change in the refraction index of the sample as a consequence of water absorption and/or presence of products formed by the hydrolytic process [49, 50]. As previously illustrated [51], the first step of bioassimilation for aliphatic polyesters is probably preceded by abiotic hydrolysis which transforms long polymeric chains in monomeric and oligomeric products, easily adsorbed by microorganisms. The disintegration test showed that all the materials were visibly disintegrated after 30 days, and a progressive darkening of the samples is clearly observed [22]. PLA matrix at 40 days is virtually disappeared as previously proved [22], and after this time only okra fibres are remaining in the tested samples. This result is confirmed by FESEM observations (Fig. 5) conducted on PLA/okra after different steps of incubation for both UOF (Fig. 5a) and ODC (Fig. 5b) based systems. At 10 days of incubation the presence of PLA matrix at the interphase with the fibres was yet evident. Starting from 20 day in composting a marked embrittlement of the PLA matrix was highlighted by FESEM observations and the presence of the only fibrous structures was detected after 30 and 40 days in composting. This effect was particular evident in the case of PLA/okra composites loaded with ODC (Fig. 5b) due to the action of water absorption that preferentially penetrates at the interphase of these systems that showed a less effective matrix/fibre interaction respect to the UOF as discuss in the morphological section. Some cracks around the interphase were observed in PLA/10ODC and PLA/20ODC yet after 10 days in composting due to the interfacial delamination and the shrinkage of matrix PLA and related to its crystallization properties [52].

The disintegrability in composting conditions was evaluated in terms of mass loss at different incubation times and the disintegration kinetics for different formulations were evaluated. The disintegration process takes place between 20 and 30 days of incubation, as reported in Fig. 6 and confirming previous discussion. The disintegrability value remains constant for all systems until 10 days of incubation, while reaches about a 60 % at 20 days and then 80 % at 30 days for all PLA based systems except for the neat PLA and PLA/30ODC that after 20 days show a disintegrability value of 20–25 % and then reach 80 % at 30 days. The

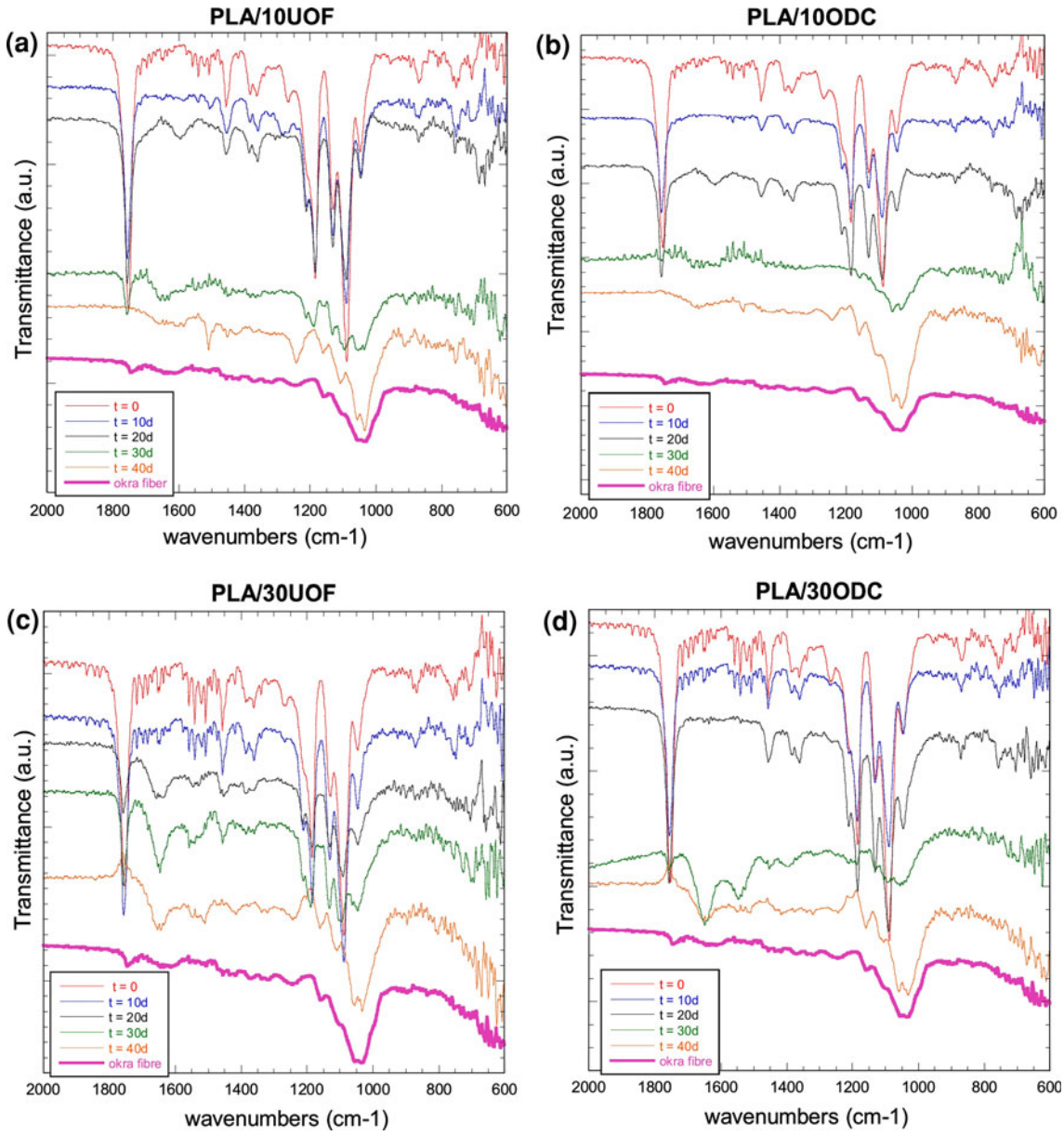

Fig. 7 ATR spectra in the 2,000–600 cm^{-1} range for PLA/10UOF (**a**), PLA/10ODC (**b**), PLA/30UOF (**c**) and PLA/30ODC (**d**) at different incubation times

induction time for starting the enzymatic degradation was quite long indicating that microorganisms required an adaptation period to produce suitable enzymes capable to break down PLA polymeric chains [53]. Moreover, the final amount of fibres after 40 days of incubation is lower than the initial value introduced in the composites for all systems, suggesting that also the fibres degrade during the process [22]. The introduction of 10 and 20 wt% of both untreated and treated fibres increase the disintegrability rate of PLA matrix due to the presence of hydroxyl groups belonging to the cellulose structure that play a catalytic role on the hydrolysis of the ester groups of the polymer. This important result suggests the possibility to induce an acceleration of PLA weight loss due to the natural fibre introduction useful for the environmental impact of these composites during their post-use [54]. Moreover, to clarify which was the chemical environment to which the samples are exposed and to confirm the possibility to use the soil for agricultural uses, compost was left to settle for 60 days after the final measurements. Total solids in the substrate were evaluated by drying a known amount at about 105 °C for 18 h, while volatile solids were measured by subtracting to the initial weight the residual quantity of ashes after incineration of the dried solid amount at 650 °C for 8 h [55]. The synthetic

biowaste properties after the biodegradation test of PLA and PLA/okra composites (data not shown) are in agreement with the standards reported in the ISO20200 suggesting the possibility to use this soil for agricultural uses.

Figure 7 shows the FTIR spectrum of the PLA/10UOF, PLA/10ODC and PLA/30UOF, PLA/30ODC samples at different incubation times. The infrared spectra of PLA/okra composites display the typical stretching of carbonyl group (–C = O) at 1,750 cm^{-1} by lactide, and the –C–O– bond stretching in the –CH–O– group of PLA at 1,182 cm^{-1}. The intensities of the –C = O bands of PLA systems show sharpening and increase after biodegradation. The changes of –C = O band are associated with the increase in the number of carboxylic end groups in the polymer chain during the hydrolytic degradation [56]. Comparing the spectra of untreated and treated okra based PLA composites at 10 wt% (Fig. 7a) and 30 wt% (Fig. 7b) for different incubation times, it can confirmed that the composites with the presence of a weak fibre/matrix interphase, as in the case of alkali treated fibres, are subjected to a faster biodegradation, showing the presence of residual okra fibre, after the PLA degradation, in shorter times. This behaviour is probably due to the size of the effective interface between the okra fibres and microbes of the burial test, that gets larger with the decrease of interface strength in ODC based composites. Moreover, the addition of higher contents of fibres into the composites causes acceleration of biodegradation due to preferential degradation of the fibres themselves.

Conclusions

Poly(lactic) acid (PLA) based biodegradable composites reinforced with okra (*A. esculentus*) fibres were successfully produced and characterized. The PLA/okra composites were prepared with several amounts of okra fibres (10, 20 and 30 wt% respect to the polymer matrix) and using both pristine and okra derived cellullose. Morphological investigation of the ODC underlined that the chemical procedure induces a decrease of the fibre diameter, while X-ray diffraction profile highlights the appearance of the cellulose II not detected for UOF. This confirms that the alkali treatment does not only result in a substantial removal of non-structural matter on okra fibres, but also in a increased stability of the cellulose structure.

The introduction of the fibres in the polymer matrix always resulted in a higher stiffness of the obtained composite system. Moreover, the addition of okra fibre to the PLA matrix led to a significant nucleation effect, which improved in turn the ability of the polymer to crystallize: this effect was more evident in the composites produced with ODC.

The introduction of 10 and 20 wt% of both untreated and treated fibres increased the disintegrability rate of PLA matrix due to the presence of hydroxyl groups belonging to the cellulose structure that play a catalytic role on the hydrolysis of the ester groups of the polymer. This result suggests the possibility to induce an acceleration of PLA weight loss due to the natural fibre introduction useful for the environmental impact of these composites during their post-use. To sum up these conclusions, this study proved the potential of okra fibres in a context of applications for biodegradable packaging and also suggested that an alkali treatment on okra fibre can have some positive effect on their use for the fabrication of composites with biopolymer matrix.

Acknowledgments The authors gratefully acknowledge the financial support from INSTM.

References

1. De Rosa IM, Kenny JM, Puglia D, Santulli C, Sarasini F (2010) Compos Sci Technol 70(1):116
2. Srinivasababu N, Mohan Rao KM, Suresh Kumar J (2009) Int. J Eng 3(4):403
3. Md Moniruzzaman, Mohd Maniruzzaman, Gafur MA, Santulli C (2009) J Biobased Mater Bio 3(3):286
4. De Rosa IM, Kenny JM, Mohd Maniruzzaman, Moniruzzaman M, Monti M, Puglia D, Santulli C, Sarasini F (2011) Compos. Sci Technol 71(2):246
5. Fortunati E, Puglia D, Monti M, Santulli C, Maniruzzaman M, Kenny JM (2012) J Appl Polym Sci. doi:10.1002/app.38524
6. Serizawa S, Inoue K, Iji M (2006) J Appl Polym Sci 100:618
7. Huda MS, Drzal LT, Mohanty AK, Misra M (2008) Compos Sci Technol 68:424
8. Lee BH, Kim HS, Lee S, Kim HJ, Dorgan JR (2009) Compos Sci Technol 69:2573
9. Plackett D (2004) J Polym Environ 12:131
10. Khondker OA, Ishiaku US, Nakai A, Hamada H (2006) Compos A 37:2274
11. Graupner N, Herrmann AS, Müssig J (2009) Compos A 40:810
12. Hu R, Lim JK (2007) J Compos Mater 41:1655
13. Masirek R, Kulinski Z, Chionna D, Piorkowska E, Pracella M (2007) J Appl Polym Sci 105:255
14. Bodros E, Pillin I, Montrelay N, Baley C (2007) Compos Sci Technol 67:462
15. Oksman K, Skrifvars M, Selin JF (2003) Compos Sci Technol 63:1317
16. Bax B, Müssig J (2008) Compos Sci Technol 68:1601
17. De Rosa IM, Iannoni A, Kenny JM, Puglia D, Santulli C, Sarasini F, Terenzi A (2011) Polym Compos 32(9):1362
18. Fischer H, Werwein E, Graupner N (2012) J Compos Mater 46:3077
19. Kirwan K, Johnson RM, Jacobs DK, Smith GF, Shepherd L, Tucker N (2007) Ind Crop Prod 26(1):14
20. López JP, Vilaseca F, Méndez JA, Franco E, Boufi S, Belhassen R, Mutjé P, Carvalho AJF, Curvelo AAS, V CIADICYP Conference, October 2008, Guadalajara, Jalisco, México
21. Juntuek P, Ruksakulpiwat C, Chumsamrong X, Ruksakulpiwat Y (2011) Adv Mater Res 410:55

22. Fortunati E, Puglia D, Santulli C, Sarasini F, Kenny JM (2012) J Appl Polym Sci 125:E562–E572. doi:10.1002/app.36839
23. Chattopadhyay H, Sarkar PB (1946) Proc Natl Inst Sci India 12:23
24. Alvarez VA, Vasquez A (2006) Compos A 37(10):1672
25. Arifuzzaman Khan GM, Shaheruzzaman Md, Rahman MH, Abdur Razzaque SM, Sakinul Islam Md, Shamsul Alam Md (2009) Fibers and Polym 10(1):65
26. Liu W, Mohanty AK, Drzal LT, Askel P, Misra M (2004) J Mater Sci 39(3):1051
27. Paiva MC, Ammar I, Campos AR, Cheikh RB, Cunha AM (2007) Compos Sci Technol 67(6):1132
28. Morán JI, Alvarez VA, Cyras VP, Vázquez A (2008) Cellulose 15:149
29. Petrova SN, Volkova IY, Zakharov AG (2004) Fibre Chem 36(6):393
30. Sgriccia N, Hawley MC, Misra M (2008) Compos A 39(10):1632
31. Pastorova I, Boon JJ, Arisz PW, Boon JJ (1994) Carbohydr Res 262:27
32. Mwaikambo LY, Ansell MP (2002) J Appl Polym Sci 84(12):2222
33. Liu D, Han G, Huang JH, Zhang Y (2009) Carbohydr Polym 75(1):39
34. Sun RC, Tomkinson J, Ma PL, Liang SF (2000) Carbohydr Polym 42:111
35. Johnson Ford EN, Mendon SK, Thames SF, Rawlins JW (2010) J Eng Fiber Fabr 5(1):10
36. Thygesen A, Oddershede J, Lilholt H, Thomsen AB, Stahl K (2005) Cellulose 12(6):563
37. Xu W, Reddy N, Yang Y (2009) Carbohydr Polym 76(4):521
38. Tripp VW, Conrad CM (1972) In Instrumental Analysis of Cotton Cellulose and Modified Cotton Cellulose. O'Connor RT (ed) Marcell Dekker Inc, New York p 339
39. Hori R, Wada M (2006) Cellulose 13:281
40. Park S, Baker JO, Himmel ME, Parilla PA, Johnson DK (2010) Biotechnol Biofuels 3:10
41. Mathew AP, Oksmanand K, Sain M (2005) J Appl Polym Sci 97:2014
42. Islam MS, Pickering KL, Foreman NJ (2010) Compos A 41:596
43. Pluta M, Galeski A, Alexandre M, Paul MA, Dubois P (2002) J Appl Polym Sci 86:1497
44. Fortunati E, Armentano I, Iannoni A, Kenny JM (2010) Polym Degrad Stab 95:2200
45. Fortunati E, Armentano I, Zhou Q, Iannoni A, Saino E, Visai L, Berglund LA, Kenny JM (2012) Carbohydr Polym 87:1596
46. Richards E, Rizvi R, Chow A, Naguib H (2008) J Polym Environ 16:258
47. Joseph PV, Joseph K, Thomas S, Pillai CKS, Prasad VS, Groeninckx G, Sarkissova M (2003) Compos A 34:253
48. Gattin R, Copinet A, Bertrand C, Couturier Y (2002) Int Biodeterior Biodegrad 50:25
49. Li S, Girard A, Garreau H, Vert M (2001) Polym Degrad Stab 71:61
50. Fortunati E, Armentano I, Iannoni A, Barbale M, Zaccheo S, Kenny JM (2011) J Appl Polym Sci 124(1):87
51. Scott G (1997) Trends Polym Sci 5:361
52. Teramoto N, Urata K, Ozawa K, Shibata M (2004) Polym Degrad Stab 86:401
53. Iovino R, Zullo R, Rao MA, Cassar L, Gianfreda L (2007) Polym Degrad Stab 93:147
54. Fukushima K, Abbate C, Tabuani D, Gennari M, Camino G (2009) Polym Degrad Stab 94:1646
55. ISO20200—Determination of the degree of disintegration of plastic materials under simulated composting conditions in a laboratory-scale test
56. Kumar R, Yakubu MK, Anandjiwala RD (2010) eXPRESS. Polym Lett 14(7):423